
Weak Disruptive Selection and Incomplete Phenotypic Divergence in Two Classic Examples of Sympatric Speciation: Cameroon Crater Lake Cichlids.
Author(s): Christopher H. Martin
Reviewed work(s):
Source: *The American Naturalist*, Vol. 180, No. 4 (October 2012), pp. E90-E109
Published by: The University of Chicago Press for The American Society of Naturalists
Stable URL: http://www.jstor.org/stable/10.1086/667586
Accessed: 14/09/2012 14:38

---

vol. 180, no. 4 the american naturalist october 2012

E-Article

Weak Disruptive Selection and Incomplete Phenotypic Divergence in Two Classic Examples of Sympatric Speciation: Cameroon Crater Lake Cichlids

Christopher H. Martin*

Department of Evolution & Ecology and Center for Population Biology, University of California, Davis, California 95616

Submitted February 2, 2012; Accepted May 21, 2012; Electronically published August 24, 2012

Online enhancement: appendix (PDF file). *Dryad data:* http://dx.doi.org/10.5061/dryad.rn30d.

abstract: Recent documentation of a few compelling examples of sympatric speciation led to a proliferation of theoretical models. Unfortunately, plausible examples from nature have rarely been used to test model predictions, such as the initial presence of strong disruptive selection. Here I estimated the form and strength of selection in two classic examples of sympatric speciation: radiations of Cameroon cichlids restricted to Lakes Barombi Mbo and Ejagham. I measured five functional traits and relative growth rates in over 500 individuals within incipient species complexes from each lake. Disruptive selection was prevalent in both groups on single and multivariate trait axes but weak relative to stabilizing selection on other traits and most published estimates of disruptive selection. Furthermore, despite genetic structure, assortative mating, and bimodal species-diagnostic coloration, trait distributions were unimodal in both species complexes, indicating the earliest stages of speciation. Long waiting times or incomplete sympatric speciation may result when disruptive selection is initially weak. Alternatively, I present evidence of additional constraints in both species complexes, including weak linkage between coloration and morphology, reduced morphological variance aligned with nonlinear selection surfaces, and minimal ecological divergence. While other species within these radiations show complete phenotypic separation, morphological and ecological divergence in these species complexes may be slow or incomplete outside optimal parameter ranges, in contrast to rapid divergence of their sexual coloration.

Keywords: adaptation, adaptive radiation, disruptive selection, selection gradient, diversification, ecological opportunity, fitness landscape, sexual selection, adaptive dynamics, trophic competition.

Introduction

After 150 years of contention, the theoretical possibility and existence in nature of at least a few plausible examples of sympatric speciation is now widely accepted (reviewed in Via 2000; Turelli et al. 2001; Coyne and Orr 2004; Gavrilets 2004; Bolnick and Fitzpatrick 2007). This endpoint on the speciation-with-gene-flow continuum is traditionally defined geographically as individuals in a population within dispersal range of each other (Mallet et al. 2009) or, from a population genetic viewpoint, as the evolution of reproductive isolation within an initially panmictic population (Fitzpatrick et al. 2008). Despite its apparent rarity in nature, dependent on both the spatial scale of gene flow (Kisel and Barraclough 2010) and the rarity of geographic scenarios in which it can be strongly inferred (Coyne and Orr 2004), sympatric speciation holds a perennial fascination due to its formidable integration of natural and sexual selection, ecology, and population genetics (Bolnick and Fitzpatrick 2007; Fitzpatrick et al. 2008). Moreover, it illustrates the power of natural selection to generate biodiversity without geographic intervention (Darwin 1859).

Models of sympatric speciation by natural selection generally require three initial conditions for the splitting of ecological subgroups within a population: (1) strong disruptive selection on ecological traits, (2) strong assortative mating by ecotype, and (3) the buildup of linkage disequilibrium between mating and ecological loci (Kirkpatrick and Ravigne 2002; Bolnick and Fitzpatrick 2007). The central requirement is that disruptive selection on ecotypes within a freely interbreeding population is strong enough to drive the evolution of nonrandom mating with respect to ecotype, thus increasing linkage between ecotype and mate choice loci and ultimately reproductive isolation between ecotypes (pleiotropic traits affecting ecotype and assortative mating can also circumvent the obstacle of linkage; Servedio et al. 2011). Disruptive selection arises either from frequency-dependent competition for shared resources (Roughgarden 1972; Bolnick 2004*a*; Pfennig and Pfennig 2010), performance trade-offs resulting from ad-

---

* E-mail: chmartin@ucdavis.edu.

Am. Nat. 2012. Vol. 180, pp. E90–E109. © 2012 by The University of Chicago. 0003-0147/2012/18004-53625$15.00. All rights reserved.
DOI: 10.1086/667586

aptation to different resources (Wilson and Turelli 1986; Martin and Pfennig 2009), or the uneven distribution of resources in the environment (Schluter and Grant 1984; Hendry et al. 2009). Genetic homogenization due to random mating is dependent on the effective recombination rate (Via 2009); the rate of decay of linkage disequilibrium (Flint-Garcia et al. 2003); the number of genetic loci underlying ecotypes, mate choice, and ecotype marker traits (Bolnick and Fitzpatrick 2007); and the strength of assortative mating (Dieckmann and Doebeli 1999; Otto et al. 2008; van Doorn et al. 2009).

Beyond these three necessary conditions, the importance of additional factors is unknown. For example, if ecotype divergence automatically results in assortative mating (Berlocher and Feder 2002) or generates some reproductive isolation as a by-product (automatic and classic magic traits sensu Servedio et al. 2011), then sympatric speciation is relatively easy (Dieckmann and Doebeli 1999). Indeed, sympatric speciation facilitated by magic traits may be common (Berlocher and Feder 2002; Sorenson et al. 2003; Papadopulos et al. 2011). In contrast, sympatric speciation should be more difficult when ecotype, species-specific markers, and mate choice loci are all initially unlinked (Dieckmann and Doebeli 1999), but the occurrence of this form of sympatric speciation in nature is unknown because it requires ruling out the presence of any magic traits, which may be very common (Servedio et al. 2011).

Additional components may also be necessary for sympatric speciation, such as sexual selection (van Doorn et al. 2009; Maan and Seehausen 2011), competition versus habitat preference (Bolnick and Fitzpatrick 2007), genomic islands of speciation (Kirkpatrick and Barton 2006; Via 2009; Michel et al. 2010), one- or two-allele mechanisms of assortative mating (Felsenstein 1981), and the shape of resource distributions and competition functions (Baptestini et al. 2009; Thibert-Plant and Hendry 2009).

There is now a plethora of theoretical models combining a range of these components and most recent models agree that sympatric divergence is plausible in some range of parameter space (Dieckmann and Doebeli 1999; Kondrashov and Kondrashov 1999; Bolnick and Doebeli 2003; Doebeli et al. 2005; Bolnick and Fitzpatrick 2007; Otto et al. 2008; Ripa 2008). However, understanding sympatric speciation in nature has been inhibited by the lack of empirical testing of parameter ranges and components present in our best case studies of this process (Gavrilets et al. 2007). Even in the most compelling examples, doubt about the population genetic conditions of initial divergence will always remain (Barluenga et al. 2006; Schliewen et al. 2006) and should continue to be addressed from new angles. However, if we take these case studies as our best estimate of the process of sympatric speciation in nature, then empirical estimates of components and parameter ranges in these systems (Gavrilets et al. 2007), relative to estimates in systems where sympatric speciation has not occurred (Bolnick 2011), can help cull the many existing theoretical models and provide realistic parameter values for future efforts. Ultimately, this approach should lead to an understanding of the necessary and sufficient components and parameter space for sympatric speciation in nature.

One complication of this retrospective approach is that speciation models estimate the initial conditions for speciation to proceed, whereas in most empirical systems, speciation is already under way or has completed. For example, models predict that strong disruptive selection is necessary to initiate sympatric speciation, but the fitness surface begins to flatten as phenotypic variance increases, resulting in weak or absent disruptive selection after phenotypic separation of ecological subgroups (Dieckmann and Doebeli 1999; Bolnick and Doebeli 2003; also see discussion of the ghost of competition past: Connell 1980). Thus, interpreting these estimates of selection additionally requires an understanding of the progress of speciation within each system; ideally, species in the earliest stages of divergence should provide the best estimates of the initial conditions of sympatric speciation.

Here I estimated the form and strength of natural selection in the flagship example of sympatric speciation, the Cameroon crater lake cichlid radiations: Coyne and Orr (2004, p. 152) state, “We know of no more convincing example [of sympatric speciation] in any group.” Indeed, the three independent sympatric radiations of Cameroon cichlids admirably fulfill Coyne and Orr’s (2004) stringent criteria for sympatric speciation: each is a monophyletic radiation of reproductively isolated species endemic to small, isolated, and uniform lake basins, precluding any historical period of allopatry (Schliewen et al. 1994, 2001; Schliewen and Klee 2004; also see Barluenga and Meyer 2010). In particular, the uniformity of the two crater lake basins of Barombi Mbo and Bermin and tiny size of Lake Ejagham (0.49 km^2) are particularly rare geographic features of any sympatric adaptive radiation (C. H. Martin and P. C. Wainwright, unpublished manuscript) that strongly suggest that any historical fluctuations in water level could not have created multiple allopatric basins (Schliewen et al. 1994). Furthermore, the sheer number of species within each radiation (11, 9, and 4 nominal species, respectively) suggests that repeated riverine speciation, crater colonization, and extinction of the riverine source population by each species is extremely unlikely (Schliewen et al. 1994; Dunz and Schliewen 2010). A more plausible alternative of repeated colonization followed by hybridization and repeated speciation of the colonists (Taylor and MacPhail 2000) is also unlikely due to the extreme isolation of these lakes; for example, many crater lakes in the same region were never colonized by cichlids (e.g., Lake Soden/Dissoni; Green 1972), and Barombi Mbo was never colonized by cladocerans, zooplankton present in most aquatic communities (Trewavas et al. 1972).

To test the prediction of strong disruptive selection before phenotypic divergence, common to all models of sympatric speciation by natural selection, I measured the current strength of nonlinear (quadratic and correlational) selection within one incipient species complex from each of two independent cichlid radiations in Cameroon, Barombi Mbo *Stomatepia* and Ejagham *Tilapia*. I used large sample sizes recommended for estimates of nonlinear selection (Kingsolver et al. 2001*a*) and introduce a method from the fisheries literature for estimating relative growth rates in cross-sectional samples from scale growth rings (Doyle et al. 1987; Fukuwaka and Kaeriyama 1997; Cheung et al. 2007). I measured selection on five functional traits, categorized species-diagnostic coloration relative to morphology, tested for phenotypic clustering and multimodality, estimated trophic divergence from stable isotope analyses, and compared the alignment of the major axes of the phenotypic variance-covariance matrix with the major axes of the nonlinear selection surface in each species complex. This study complements previous work on these adaptive radiations that focused on their population genetics, taxonomy, and monophyly (Trewavas et al. 1972; Schliewen et al. 1994, 2001; Schliewen and Klee 2004; Dunz and Schliewen 2010; Neumann et al. 2011). Despite the importance of these classic model systems in evolution and ecology (Kocher 2004; Seehausen 2006), to my knowledge, this study represents the first field estimate of natural selection in any African cichlid (also see Albertson et al. 2003; Swanson et al. 2003).

Methods

Study System

I sampled only from Lakes Barombi Mbo and Ejagham due to the difficulty of obtaining permission from the local community to work in Lake Bermin. Barombi Mbo is a volcanic crater lake, 2.3 km in diameter and at least 1 million years old (Cornen et al. 1992), with a few seasonal inflowing streams and one outlet flowing down an elevation gradient. The crater reaches a depth of 110 m, but the normoxic zone extends to only 40 m (Trewavas et al. 1972; Schliewen et al. 1994). This lake contains a monophyletic radiation of cichlid species derived from a riverine lineage of the tilapiine cichlid *Sarotherodon galilaeus* (Schliewen et al. 1994). Eight of these cichlid species coexist in the approximately 30-m-wide littoral zone along the steeply sloping crater rim to depths of around 5 m; three additional cichlid species occur in deepwater and open-water habitats. I targeted the closely related species *Stomatepia mariae* and *Stomatepia pindu* because they closely overlap in habitat and diet: both are exclusively found together in the littoral zone and feed predominantly on aquatic arthropods; *S. mariae* sometimes includes more floating terrestrial insects in its diet (Trewavas et al. 1972). A third species, *Stomatepia mongo*, is also known from the lake, but was never encountered and due to its extreme rarity (6 individuals collected in the past 11 years; C. Dening, personal communication) may be restricted to lower depths or is critically endangered. The phylogenetic relationship among these three species is unresolved, but they form a well-supported clade within the Barombi Mbo cichlid radiation (Schliewen et al. 1994; Schliewen and Klee 2004). Two individuals within each of the three *Stomatepia* species also group together in an amplified fragment length polymorphism (AFLP) phylogeny (maximum likelihood bootstrap support ≥99%; Schliewen and Klee 2004), indicating at least some reproductive isolation among these species. The main diagnostic feature, for both scientists and local fishermen, is coloration: *S. pindu* (Barombi name: pindu) are dark brown to black throughout their body with a blotchy black stripe, and breeding males turn coal black; *S. mariae* (Barombi name: nsess) are light gray with a crisp black stripe, and breeding males take on a metallic green sheen; additional divergent morphological characters including head depth and stomatal pore openings are noted in their species descriptions (Trewavas et al. 1972). *Stomatepia pindu* generally defend territories closer to the leaf litter, while *S. mariae* occupy fallen logs higher in the water column, but adults and juveniles of both species show extensive depth and habitat overlap. A total of 572 *S. mariae* and *S. pindu* were collected from a single 100-m stretch of the littoral zone minimally impacted by erosion (although swidden agriculture is practiced along the entire crater rim) in habitat dominated by fallen logs, branches, and leaf litter without macrophytes or silt deposition, the dominant habitat in this zone. For morphological comparison to the study site, an additional 76 *Stomatepia* were collected from three additional sites along the entire crater rim, spanning the range of littoral habitats within the lake.

Lake Ejagham is a younger (10,000–100,000 years old), nonvolcanic solution basin (D. Livingstone, personal communication, in Schliewen et al. 2001), only 900 × 630 m wide and 17 m deep (Kling 1988) with no inflowing streams and a single outflowing seep into the forest. Remarkably, this tiny lake contains two endemic radiations of cichlids, the sister species *Sarotherodon knauerae* and *Sarotherodon lamprechti* (Neumann et al. 2011) and at least four species of *Tilapia* (*Coptodon*) derived from a riverine lineage of the tilapiine cichlid *Tilapia* (*Coptodon*) sp. ‘Cross’ (Dunz and Schliewen 2010). I targeted the abundant *Tilapia* species complex that occurs throughout the lake. Juveniles are highly variable and cannot be assigned to species, but breeding pairs of three species were observed substrate spawning along the shoreline and showed complete assortative mating (*Tilapia fusiforme*, $n = 31$; *Tilapia deckerti*, $n = 24$; *Tilapia ejagham*, $n = 2$). *Tilapia deckerti* adults are deeper bodied with red ventral breeding coloration, *T. fusiforme* is elongate with solid black breeding coloration, and *T. ejagham* reaches the largest size in the lake with greenish breeding coloration (additional description in Dunz and Schliewen 2010). *Tilapia deckerti* pairs defended territories within twigs or leaf litter while *T. fusiforme* defended crevices within logs or under fallen wood; spawning pairs of each species were completely interspersed along the shoreline, generally guarding territories in water less than 1 m deep. *Tilapia ejagham* reached a larger size before breeding and pairs defended territories in slightly deeper water at depths of around 1.5–2 m. No dietary information for these species has been published, but *T. fusiforme* generally occurred higher in the water column, suggesting a limnetic diet, while *T. deckerti* generally remained closer to the substrate, suggesting a benthic diet. *Tilapia ejagham* (provisionally known as *Tilapia* sp. 'predator'; Schliewen et al. 2001) may include more small fishes in its diet (Dunz and Schliewen 2010). A fourth species, *Tilapia nigrans*, is reported only from deepwater scuba transects below 5 m (Dunz and Schliewen 2010) and may not be present in my sample. A total of 523 *Tilapia* were collected from five different sites around the lake (due to the smaller size of Lake Ejagham), each comprising similar littoral habitat of leaf litter and fallen branches lacking macrophytes. An additional 50 breeding individuals of *T. deckerti* and *T. fusiforme* guarding spawning sites, eggs, or fry were collected in situ using a barrier net and hand net for comparison of breeding coloration and morphology.

Morphometrics

Fishes were collected between December 28, 2009, and January 18, 2010, using a 5-m seine net with 0.5-cm^2 mesh size supplemented by gill nets and barrier nets, allowing for capture of large adults as well as large juveniles (standard length [SL] range: 2.75–10.09 cm, Barombi Mbo; 2.45–9.52 cm, Ejagham). Hook-and-line fishing was also used to target the larger *T. ejagham* individuals in Lake Ejagham. Captured fishes were euthanized in an overdose of MS-222, labeled, and stored in 95% ethanol. Each specimen was photographed on the left lateral side using a Canon EOS digital SLR, and linear distances of functional traits were measured from digital images, using ImageJ (National Institutes of Health). Ecologically relevant traits were chosen that were most likely to morphologically discriminate species within each complex based on initial observations and species descriptions (Trewavas et al. 1972; Dunz and Schliewen 2010). Body depth was measured from the insertion of the first dorsal ray to the ventral surface, perpendicular to the major axis of the fish. Head depth was measured from the insertion of the epaxial muscle on the dorsal surface of the neurocranium to the ventral surface, perpendicular to the major axis of the fish. Lower jaw length was measured from the center of the protruding quadrate-articular joint on the external jaw line to the tip of the most anterior tooth on the mandible. The ascending process of the premaxilla links rotation of the dorsal process of the maxilla to forward jaw protrusion in cichlids (Motta 1984) and was measured from its dorsal tip, which visibly distended the skin along the rostrum, to the tip of the most anterior tooth on the dentigerous arm of the premaxilla. Orbit diameter was measured along the horizontal and vertical axes of the fish and averaged. Finally, the SL of all specimens was measured using dial calipers.

Residuals from a linear regression of log-transformed trait and log-transformed SL were used for all analyses (performed separately for each species complex). Although SL distributions were skewed rightward in both species complexes, excluding the largest individuals from each sample to eliminate skew before calculating residuals had no qualitative effect on estimates of selection gradients (table S1, available online), and all individuals were included in subsequent analyses.

Model-based clustering analysis was used to assess the number of groups within each species complex based on the five size-corrected traits measured. Bayesian information criterion scores (BIC; Schwarz 1978) were used to choose among multivariate normal mixture models incorporating from 1–9 clusters and varying covariance structures with the R package MCLUST (ver. 3; Fraley and Raftery 2007). Uncertainty of group assignment in the best model was then evaluated by counting the percentage of the sample assigned to a cluster with less than 95% probability and less than 80% probability (Fraley and Raftery 2007). Multimodality of all trait distributions was also inspected visually and tested using Hartigan's dip test for multimodality (Hartigan and Hartigan 1985).

Species-Diagnostic Coloration

For Barombi Mbo *Stomatepia*, it was possible to categorize most collected individuals (both breeding and nonbreeding adults and juveniles) according to their species-diagnostic melanin coloration (without regard to morphology). *Stomatepia mariae* coloration ($n = 168$) was defined as an unbroken, crisp black stripe on a light background, whereas *S. pindu* coloration ($n = 324$) was defined as a blotchy, broken black stripe on a dark background. Some individuals could not be assigned to either category and were labeled as ambiguous ($n = 80$).

Ejagham *Tilapia* displayed species-diagnostic coloration only while guarding breeding territories. Breeding individuals ($n = 50$) were photographed in the field immediately following euthanasia with an overdose of MS-222. *Tilapia fusiforme* coloration was defined by solid black coloration, whereas *T. deckerti* coloration was defined by a red ventral region and olive dorsal surface.

Stable Isotope Analyses of Diet

Trophic divergence was estimated from stable isotope ratios of δ^{13}C, indicating relative sources of benthic and limnetic carbon, and δ^{15}N, indicating relative trophic position within lakes (Post 2002). Representatives of each species complex (Barombi Mbo *Stomatepia*, $n = 13$ from the 100-m study site; and Ejagham *Tilapia*, $n = 50$ from two neighboring sites) and a trophic specialist species in Barombi Mbo (*Pungu maclareni*, $n = 6$ from the study site) were sampled. Immediately following euthanasia, approximately 5 mg of white muscle tissue was removed from the caudal peduncle of each specimen and dehydrated in individual sealed containers in the field using the desiccant magnesium perchlorate. In the laboratory, dehydrated samples were dried at 60°C for 24 hours, weighed, and sent to the University of California, Davis, Stable Isotope Facility for measurement on a PDZ Europa ANCA-GSL elemental analyzer interfaced to a PDZ Europa 20-20 isotope ratio mass spectrometer (Sercon, Cheshire, UK).

Fitness Estimates: Scale Circuli Spacing

Trophic competition has been proposed as the major mechanism driving species diversification in Cameroon cichlids since sister species differ largely in trophic traits with very little sexual dimorphism (Schliewen et al. 1994; Coyne and Orr 2004) unlike the larger haplochromine cichlid radiations of east Africa (Streelman and Danley 2003; Martin and Genner 2009). Therefore, relative growth rates, which provide an estimate of fitness due to differential foraging success among individuals (Bolnick and Lau 2008), are an ideal fitness proxy for testing speciation driven by resource competition.

To estimate relative growth rates, I measured the signature of growth contained in the spacing of scale circuli for each specimen. Fishes add distinct bony ridges to the interior margin of each scale as they grow, known as scale circuli (Kobayashi 1961; Doyle 1987; Cheung et al. 2007). Circuli are deposited daily in young juveniles but less often as the fish ages (Szedlmayer et al. 1991; Kingsford and Atkinson 1994), and the number of scale circuli is correlated with age (Kingsford and Atkinson 1994). Importantly, increased growth rates are correlated with larger spacing between each circulus, allowing for estimates of growth rate from cross-sectional samples in taxa where longitudinal studies are nearly impossible, such as Cameroon cichlids. The correlation between scale circuli spacing and growth rate has been widely validated in commercial species (Kobayashi 1961; Bilton 1975; Fisher and Pearcy 1990, 2005; Fukuwaka and Kaeriyama 1997; Cheung et al. 2007), including two African cichlids, *Oreochromis mossambicus*/*hornorum* (Doyle 1987) and *Hemichromis bimaculatus* (Sire 1986). Furthermore, scale circulus spacing has been linked to survival rates in the wild (Healey 1982). Similar to all other species reported, the correlation between scale circuli spacing and growth rate was high in African cichlids, ranging from $r = 0.65$–0.75 in populations of mixed brood, age, and size, similar to natural field conditions (Doyle 1987). Additionally, one study found scale circuli were more strongly correlated with growth ($r = 0.79$) than RNA : DNA ratios ($r = 0.22$; Cheung et al. 2007), a leading biochemical indicator of growth rate (Buckley 1984; Bolnick and Lau 2008). While RNA : DNA ratios can change significantly within 2 weeks (Svänback and Bolnick 2007), each scale circulus is deposited over several days in adult fishes (unlike daily otolith increments), and the spacing of each ridge provides a lasting anatomical record of past growth rates (Healey 1982; Sire and Arnulf 2000). Scale circulus spacing may also indicate life-history transitions, such as shifts in the natal environment (Barlow and Gregg 1991; Ibanez et al. 2008) or marine migrations (Hubley et al. 2008) but not toxin exposure or hypoxia (Cheung et al. 2007).

To further validate this approach for Cameroon cichlids, I raised 31 *Tilapia* (*Coptodon*) *snyderae* in laboratory aquaria at 24°–25°C for 1 month. While Barombi Mbo *Stomatepia* and Ejagham *Tilapia* are normally not commercially available, *T. snyderae* is frequently traded and is closely related (Schliewen et al. 1994; Schliewen and Klee 2004). *Tilapia snyderae* originates from the third adaptive radiation of Cameroon tilapiine cichlids in crater lake Bermin (Stiassny et al. 1992; Schliewen et al. 1994) and thus provides a highly similar comparison to field-collected specimens due to both shared history and ecology. Captive-raised individuals of varying sizes (SL range: 4.18–8.26 cm) from multiple broods were kept singularly and in groups and randomly assigned to either low-feeding (approximately once per week) or high-feeding (daily ad lib.) treatments. Growth rate per day was measured from the log-transformed difference in SL at the start and at the end of feeding treatments, terminated after 36 days for most individuals (several individuals expired before the end of the study and were included in analyses). Individuals were then euthanized and scale circuli spacing was measured as described below.

For all field-collected and lab-raised specimens, the first three fully formed scales posterior to the pelvic girdle were removed from the first scale row dorsal to the lateral line on the right side of each specimen. These scale positions were identical among species from all three crater lakes so that homologous scales could be measured in each case. If any of the first three scales was missing or not fully formed, the fourth or fifth scale was measured in its place (there was no major difference in circuli spacing among these scale positions relative to the ranges observed across individuals: Barombi scale positions 1–5 (mean pixels ± SE): 44.8 ± 0.59, 42.5 ± 0.55, 42.2 ± 0.55, 42.7 ± 0.56, 44.1 ± 0.58; individual range: 26–105; Ejagham scale positions 1–5: 42.2 ± 0.42, 41.5 ± 0.42, 40.3 ± 0.40, 40.4 ± 0.39, 40.3 ± 0.39; individual range: 26–76). Scales were mounted on a microscope slide with glycerin and photographed at ×40 using an Olympus CH30 compound microscope with Microsoft LifeCam software and a USB camera. Each cycloid scale contained distinct columns of scale circuli on its embedded margin (fig. 1). The linear distance between the five most recent scale circuli was measured using ImageJ for at least three columns per scale and averaged, beginning with the most ventral column on each scale (fig. 1*c*). This was repeated for at least three scales per fish. All scale circuli were measured by a single observer (S. Romero) who was blind to trait data for each specimen.

Selection Analyses

I used Lande and Arnold's (1983) ordinary least squares regression approach to measure the form and strength of selection gradients on functional traits. Disruptive selection is indicated by positive quadratic coefficients in the linear model and the presence of a fitness minimum within the population; conversely, stabilizing selection is indicated by negative quadratic coefficients and the presence of a fitness maximum within the population (Kingsolver and Pfennig 2007). To remove the effects of size from each trait and relative growth rates, residuals from a linear regression of log-transformed trait and log-transformed SL were used for analyses (performed separately for each species complex). Relative growth rate residuals and trait residuals were then standardized to a standard deviation of unity to enable comparison of parameter values across systems (Kingsolver et al. 2001*a*). There was no nonlinear scaling between relative growth rate residuals and log-transformed SL in Ejagham *Tilapia* (quadratic term, $P = .61$). In Barombi Mbo *Stomatepia*, a cluster of high-growth individuals ($n = 45$) larger than 4.2 cm SL resulted in a negative quadratic relationship between relative growth rate residuals and log-transformed SL (quadratic term, $P = .002$). However, dividing the data set into large (>4.2 cm SL) and small individuals (≤4.2 cm SL) eliminated nonlinear scaling between growth rate residuals and log-transformed SL (each quadratic term, $P > .05$). Selection coefficients for large individuals were qualitatively similar to the full data set (table S2, available online), and the full data set was used for all subsequent analyses.

The matrix of quadratic and correlational selection gradients (γ) for each species complex was estimated from quadratic regression using the lm function in R (R Development Core Team 2011). To facilitate comparison with previous studies, the vector of directional selection gradients (β) was estimated separately in a first-order regression rather than within the full quadratic model (Blows and Brooks 2003). Quadratic coefficients from the re-

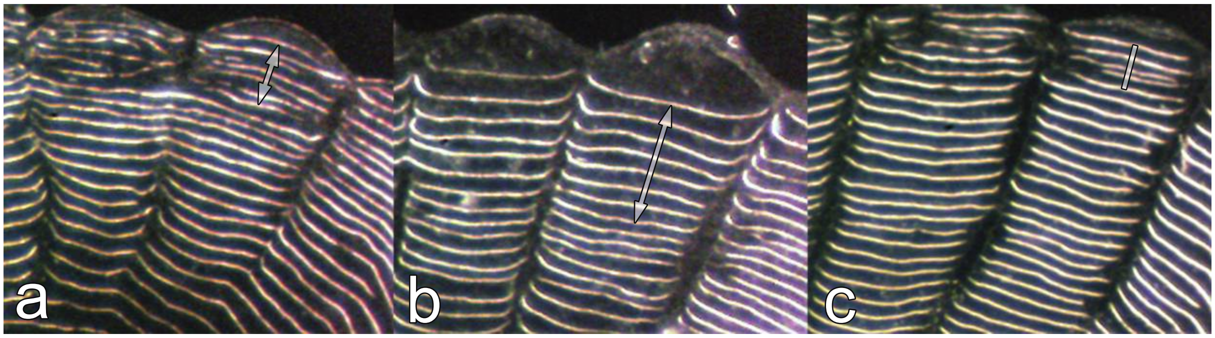

Figure 1: Scale circulus spacing on the embedded margin of cycloid scales indicating relative growth rates in Cameroon cichlids. Laboratory-raised *Tilapia snyderae* were exposed to different feeding regimes for 5 weeks: *a*, restricted weekly feedings corresponded to reduced scale circuli spacing (span of treatment approximated by white arrow) with a shift in spacing indicating the start of treatment; *b*, daily ad lib. feedings corresponded to increased scale circulus spacing (approximated by white arrow); and *c*, wild-caught *Stomatepia* sp. scale margin indicating a recent period of reduced growth. The white bar indicates the increment of 5 scale circuli measured on at least three columns per scale and three scales per fish as a proxy for growth rate in all selection analyses.

gression model were doubled for quadratic selection gradients (Stinchcombe et al. 2008). Fitness surfaces were also visualized using thin-plate splines to determine whether quadratic models were adequate (Schluter and Nychka 1994; Blows and Brooks 2003). Each multivariate spline was fit to the five size-corrected traits and relative growth rates with the Fields package in R (Fields Development Team 2006) using generalized cross validation to choose the smoothness penalty.

To assess confidence in the selection gradient estimates, I used a mixed-model approach to take advantage of the greater power provided by accounting for variation across scales within each individual. Using the lmer function from the lme4 package in R (Bates et al. 2012), log-transformed relative growth rates were estimated from the fixed linear, quadratic, and interaction effects of all five log-transformed traits and SL. The random effect of individual was also included in the model with varying intercepts. In a mixed-model design it is inappropriate to estimate P values for fixed effects because the ratio of sums of squares may not approximate an F distribution (Bates 2006; Bates et al. 2012); instead, Markov Chain Monte Carlo (MCMC) sampling from the fitted model can be used to estimate posterior probability densities of model parameters (Bates et al. 2012). Bayesian credible intervals constructed from the highest posterior densities indicate support for model parameters if the intervals do not contain zero at a given confidence range. These credible intervals should generally be more conservative (larger) than frequentist confidence intervals because MCMC sampling allows all parameters within the model to vary rather than conditioning on fixed estimates. I examined 95%, 99%, 99.9%, and 99.99% credible intervals for all model parameters using the functions mcmcsamp and HPDinterval in lme4 (Bates et al. 2012).

Examining nonlinear selection along only the set of measured univariate trait axes ignores quadratic selection along multivariate trait axes (Phillips and Arnold 1989; Blows and Brooks 2003). Therefore, to find the multivariate axes of highest quadratic curvature relative to growth rate, I performed canonical rotation of the standardized trait values and relative growth rates using the rsm package in R (Lenth 2009). This procedure generates a new set of multivariate axes, with all correlational selection between traits removed, in which the eigenvalue of each eigenvector represents the nonlinear selection gradient along that axis (Phillips and Arnold 1989; Blows and Brooks 2003). This new set of axes can be understood as the principal components of the nonlinear selection surface (Arnold et al. 2001). Confidence in these parameters can then be assessed by placing these rotated axes back into a quadratic regression model with log-transformed relative growth rates as response variable and examining P values for each canonical axis (Simms and Rausher 1993; Blows and Brooks 2003; no mixed-model approach is available for canonical analysis).

Alignment of the Selection Surface and the **P** *Matrix*

To further explore phenotypic constraint in these two species complexes, I compared the alignment of the major axes of the nonlinear selection surface (eigenvectors of the canonical response surface: $\mathbf{M}_{1-5}$) with the major axes of the phenotypic variance-covariance matrix **P** (the first three eigenvectors from a principal components analysis). Phenotypic divergence between species may be constrained by the major axes of the genetic variance-covariance matrix (**G**) within the diverging population, known as the genetic lines of least resistance (Schluter 1996). The major axes of **G** can influence the rate and direction of trait evolution (Lande 1979; Lande and Arnold 1983); conversely, linear and quadratic selection can also shape the **G** matrix over time (Turelli 1988; Arnold et al. 2008), sometimes quite rapidly (Blows and Higgie 2003; Doroszuk et al. 2008). In either case, increased phenotypic constraint can be inferred when the major axes of **G** are out of alignment with the major axes of the selection surface (Schluter 1996).

There are several methods for comparing the architecture of the **G** matrix and the selection surface (Steppan 2002; Blows et al. 2004; Hansen and Houle 2008). Here I used a pairwise approach of comparing the alignment of each major axis of the nonlinear response surface (from canonical rotation of the γ matrix: $\mathbf{M}_{1-5}$) with each major axis of the **P** matrix (the first three principal component axes: $\mathbf{P}_{1-3}$), modified from the approaches of Schluter (1996) and Blows et al. (2004). The **P** matrix often provides an adequate, and possibly more accurate, approximation of the **G** matrix than estimating genetic variance and covariance directly from parent-offspring relationships (Cheverud 1988; Steppan et al. 2002; Kolbe et al. 2011). Rather than focusing only on $\mathbf{P}_{\max}$ (Schluter 1996), I retained the first three principal component axes of the **P** matrix, dropping the remaining two eigenvectors based on scree plots, and compared their alignment with each of the five major vectors of the response surface ($\mathbf{M}_{1-5}$). For each pairwise comparison, I calculated the sine of the angle between the two unit vectors ($\sin\theta$) from their cross product, which varies between 0 when the two vectors are parallel and 1 when the two vectors are perpendicular. I bootstrapped ($n = 10{,}000$) the **P** matrix with replacement to generate a distribution of eigenvectors for each of the first three principal components ($\mathbf{P}_{1-3}$) and calculated the empirical 95% confidence interval of $\sin\theta$ for each pairwise comparison between $\mathbf{P}_{1-3}$ and the fixed estimates of the five major vectors of the nonlinear response surface ($\mathbf{M}_{1-5}$).

To assess confidence in these estimates, I also calculated the expected 95% confidence intervals of $\sin\theta$ for parallel

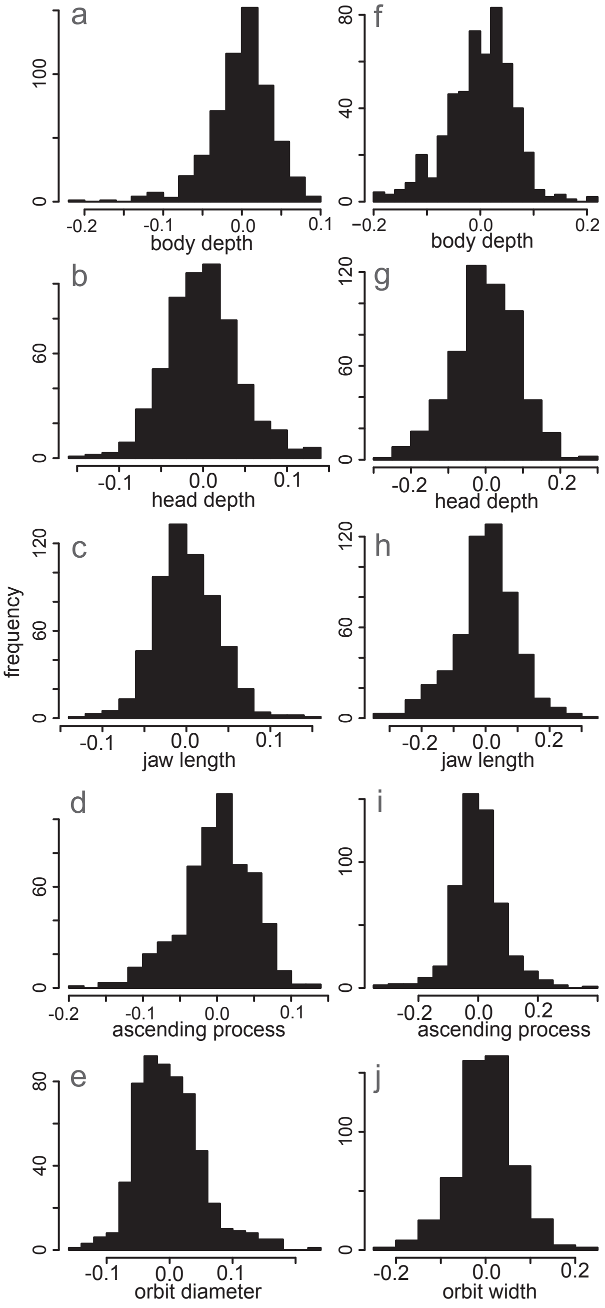

Figure 2: Trait histograms for all traits measured in Barombi Mbo *Stomatepia* (*a*-*e*) and Ejagham *Tilapia* (*f*-*j*). Traits were size corrected by taking the residuals from a linear regression of log-transformed trait on log-transformed standard length, performed separately for each species complex. Outliers were checked for accuracy.

vectors. The bootstrapped distribution for each principal component of **P** was compared to the original principal component of **P** to generate a confidence interval of sin θ, representing the expected interval if two vectors are parallel. The distribution of sin θ for each pairwise comparison between **P** and **M** vectors was then compared to the expected interval of sin θ for parallel vectors. For example, $\mathbf{P}_1$ was considered to be parallel with $\mathbf{M}_1$ if the 95% confidence interval of sin θ between $\mathbf{P}_1$ and $\mathbf{M}_1$ overlapped the expected 95% confidence interval of sin θ for parallel vectors (bootstrapped estimates of $\mathbf{P}_1$ relative to the observed vector $\mathbf{P}_1$).

Results

Morphometrics

Within each species complex, Bayesian cluster analysis identified two ellipsoidal clusters of equal shape as the best model explaining the data (Barombi Mbo *Stomatepia* ΔBIC: -50 relative to the next-best model with 3 clusters, -57 relative to the best model with 1 cluster; fig. S1, available online; Ejagham *Tilapia* ΔBIC: -48 relative to the next-best model with 3 clusters, -87 relative to the best model with 1 cluster; fig. S2). Including *Stomatepia* individuals ($n = 76$) from three additional sites in Barombi Mbo did not alter support for two ellipsoidal clusters of equal shape as the best model (ΔBIC: -72 relative to the next-best model with 3 clusters; ΔBIC: -57 relative to the third-best model with 5 clusters; fig. S3).

However, uncertainty in the probability of assignment to each cluster was greater than 0.05 in 50% of Barombi Mbo *Stomatepia* individuals and 66% of Ejagham *Tilapia* individuals measured. Similarly, uncertainty was greater than 0.20 in 15% of Barombi Mbo *Stomatepia* and 20% of Ejagham *Tilapia* (also see figs. S4 and S5 for biplots of cluster assignment in each species complex).

All traits examined exhibited a unimodal distribution within each species complex (fig. 2). Unimodality was also supported when examining histograms of Bayesian cluster assignment for each trait: the two clusters did not correspond to separate peaks for any trait (fig. S6). The null hypothesis of one mode could not be rejected for any of the five size-corrected traits or SL in either species complex (Hartigan's dip test for multimodality: $D =$ 0.0085–0.0178, $P \geq .23$).

Species-Diagnostic Coloration

In contrast to functional traits, species-diagnostic coloration was bimodal in both Barombi Mbo *Stomatepia* and breeding individuals of Ejagham *Tilapia* and corresponded to divergent morphologies (fig. 3). Most *Stomatepia* individuals collected were intermediate in morphology, but 86% could be unambiguously assigned to *Stomatepia pindu* or *Stomatepia mariae* coloration categories (fig. 3*a*). These coloration categories only partially overlapped on

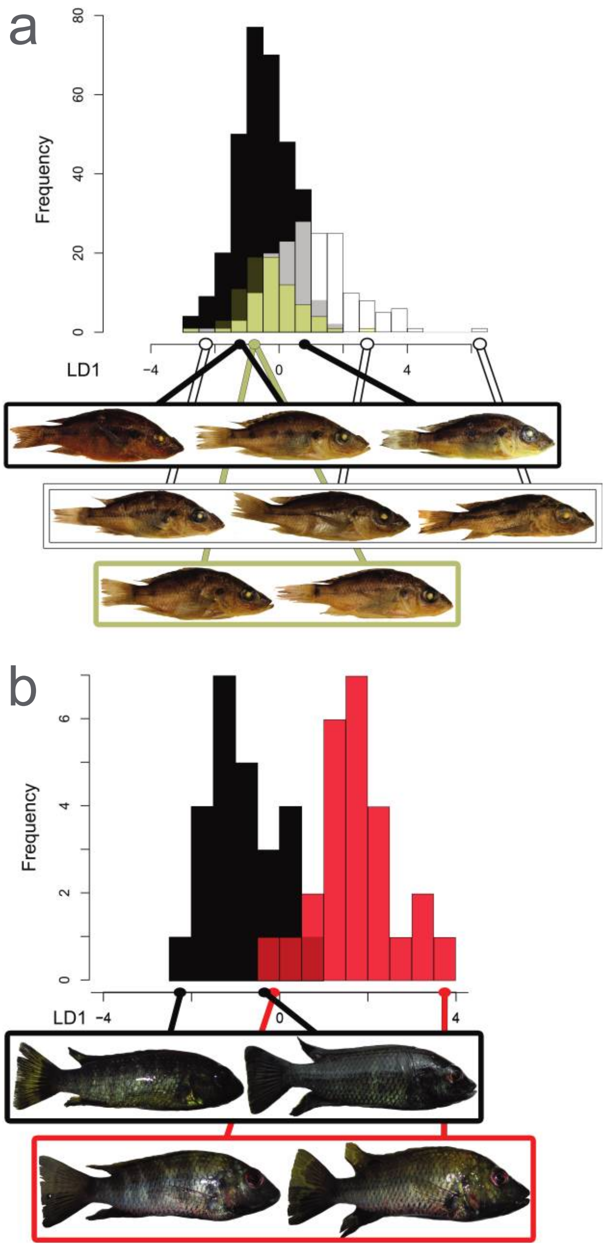

Figure 3: Overlapping histograms of species-diagnostic coloration plotted against the morphological linear discriminant axis for these two color categories applied to the five size-corrected traits measured in Barombi Mbo *Stomatepia* (*a*) and Ejagham *Tilapia* (*b*). Representative specimens of each color category are depicted and mapped to their corresponding location on the morphological discriminant axis. All Barombi Mbo *Stomatepia* collected ($n = 572$) were categorized by their species-diagnostic melanin coloration: a blotchy, broken black stripe on a dark background (*Stomatepia pindu* coloration: black); an unbroken, crisp black stripe on a light background (*Stomatepia mariae* coloration: white); or ambiguous (olive). Only breeding Ejagham *Tilapia* ($n = 50$) displayed species-diagnostic coloration of solid black (*Tilapia fusiforme* coloration: black) or red ventral and olive dorsal coloration (*Tilapia deckerti* coloration: red).

a morphological linear discriminant axis (fig. 3*a*) and showed significant morphological differences across the five traits measured relative to color (MANOVA $F_{2,569} = 21.3$, $P < .0001$). Breeding individuals of Ejagham *Tilapia* (*Tilapia fusiforme* and *Tilapia deckerti*) were distinctly bimodal in morphology with very little overlap on a morphological linear discriminant axis (fig. 3*b*) and showed significant morphological divergence by color (MANOVA $F_{1,48} = 37.1$, $P < .0001$).

Stomatepia individuals sometimes displayed the species-diagnostic coloration of one species and the extreme morphology of the other (fig. 3*a*). This decoupling of color and morphology indicates the absence of strong genetic linkage or pleiotropy between these traits and demonstrates that species-diagnostic coloration is not a magic trait in Barombi Mbo *Stomatepia*. Species-diagnostic coloration and morphology were more strongly correlated in the two species of Ejagham *Tilapia*; however, some overlap in morphology between the color categories also suggests a lack of strong linkage (fig. 3*b*).

Stable Isotope Analyses of Diet

Barombi Mbo *Stomatepia* with *mariae* and *pindu* coloration were not trophically divergent. *Stomatepia* species, defined by coloration, were not significantly different in either their limnetic-benthic carbon sources or relative trophic position (MANOVA, $F_{2,10} = 0.85$, $P = .46$; mean ± SE: -26.81 ± 0.49 and -27.48 ± 0.35 δ^{13}C; 10.23 ± 0.17 and 10.57 ± 0.19 δ^{15}N, respectively). Furthermore, the mean dietary divergence in carbon source and trophic position between *Stomatepia* species (0.66 δ^{13}C and 0.34 δ^{15}N) was, respectively, 5.6 and 2.3 times less than the mean dietary divergence between *Stomatepia* and *Pungu maclareni* (5.63 δ^{13}C and 0.78 δ^{15}N), a specialized spongivore.

Similarly, breeding individuals of Ejagham *T. fusiforme* obtained slightly more of their carbon from limnetic sources (-29.45 ± 0.17 δ^{13}C) than *T. deckerti* breeding individuals (-28.43 ± 0.14 δ^{13}C; Welch's two-tailed $t = -4.62$, $P = .00003$), but showed no difference in relative trophic position (8.69 ± 0.10 and 8.68 ± 0.12 δ^{15}N; Welch's two-tailed $t = 0.07$, $P = .94$).

Fitness Estimates: Scale Circuli Spacing in Lab-Raised and Field-Collected Specimens

Size-corrected scale circuli spacing was significantly correlated with growth rate ($r = 0.54$, df = 29, $P = .0016$) in lab-raised individuals of the Cameroon crater lake cichlid *Tilapia snyderae*. Five weeks of laboratory growth corresponded to approximately 7 scale circulus increments in both high-feeding and low-feeding treatments (fig. 1*a*, 1*b*), suggesting that growth rate measured in field samples re-

Table 1: Standardized directional selection gradients (β) and matrix of standardized quadratic and correlational selection gradients (γ) for species complexes in each lake

	β	Body depth	Head depth	Jaw length	Ascending process	Orbit diameter
Lake Barombi Mbo *Stomatepia pindu*/*mariae*:						
Body depth	**−.07***	**−.21******				
Head depth	−.03	.04	**.05***			
Jaw length	−.11	**−.01**[a]	**−.09***	−.02		
Ascending process	**.08***	−.02	**.08***	.08	**−.02**[a]	
Orbit diameter	**−.12******	.01	.05	.07	−.05	.01
Lake Ejagham: *Tilapia* (*Coptodon*)*deckerti*/*fusiforme*/*ejagham*:						
Body depth	**.41******	**.10***				
Head depth	−.01	**−.11***	.04			
Jaw length	−.04	**−.06***	−.10	.04		
Ascending process	**−.13****	−.05	**.16****	.04	**−.16******	
Orbit diameter	−.03	.06*	.06	−.11	−.04	−.006

Note: β and γ were estimated in separate regressions. Boldface indicates that the Bayesian credible interval of the parameter estimated from the linear mixed-effect model does not contain zero.

* 95% of highest posterior density.

** 99% of highest posterior density.

*** 99.9% of highest posterior density.

**** 99.99% of highest posterior density.

[a] Sign of mixed-model parameter estimate was opposite to the ordinary least squares parameter estimate shown.

flected at least the previous month of growth (fig. 1*c*). Average scale circuli spacing ranged from 26 to 76 in Ejagham *Tilapia* and 26 to 105 in Barombi Mbo *Stomatepia* field-collected specimens (in relative units at ×40 magnification, approximately 25–100 μm), more than spanning the range of scale circuli spacing resulting from once per week and daily feedings in the laboratory (range: 36–62).

Selection Analyses

The full quadratic model of size-corrected traits explained 7.3% of the variation in scale circuli spacing in Barombi Mbo *Stomatepia* ($F_{20,551} = 2.17$, $P = .002$) and 19.9% of the variation in Ejagham *Tilapia* ($F_{20,502} = 6.24$, $P < .0001$). In mixed-model analyses, the random effect of individual explained 75.1% and 55.3% of the total variation in scale circuli spacing in Barombi Mbo and Ejagham, respectively.

Significant disruptive, stabilizing, and correlational selection was present in both species complexes (table 1; fig. 4). Major nonlinear axes of the selection surface were often saddles and most individuals in the population resided within the bowl of each saddle, rather than clustering around distinct peaks (fig. 4), reflecting the lack of bimodality within each population.

Lake Barombi Mbo *Stomatepia* experienced disruptive selection on head depth and the interaction between jaw length and head depth (fig. 4; table 1). Mixed-model analysis also identified disruptive selection on the ascending process (all positive quadratic selection gradients in the 95% credible interval), but ordinary least squares regression estimated weak stabilizing selection on this trait (table 1). Lake Ejagham *Tilapia* experienced disruptive selection on the correlation between the ascending process and head depth and positive quadratic selection for body depth (but not disruptive because the fitness minimum did not occur within the range of trait values observed in the population [Kingsolver and Pfennig 2007]; fig. 4; table 1).

Canonical rotation of the response surface revealed slightly higher estimates of stabilizing and disruptive selection along the new set of multivariate axes (table 2). Both trait and canonical estimates of quadratic selection gradients were not particularly high when compared to the distribution of standardized quadratic selection gradients published in the literature (fig. 5). For example, 51% of published estimates of positive quadratic selection ($n = 226$; Kingsolver et al. 2001*b*) were equal to or greater than the highest estimate of positive quadratic selection observed in this study ($2\gamma = 0.10$; table 1).

Alignment of the Nonlinear Selection Surface and the ***P*** *Matrix*

None of the five major axes of the nonlinear response surface ($\mathbf{M}_{1\text{–}5}$) were aligned with any of the first three principal component axes of the phenotypic variance-covariance matrix ($\mathbf{P}_{1\text{–}3}$) in either species complex (table 3).

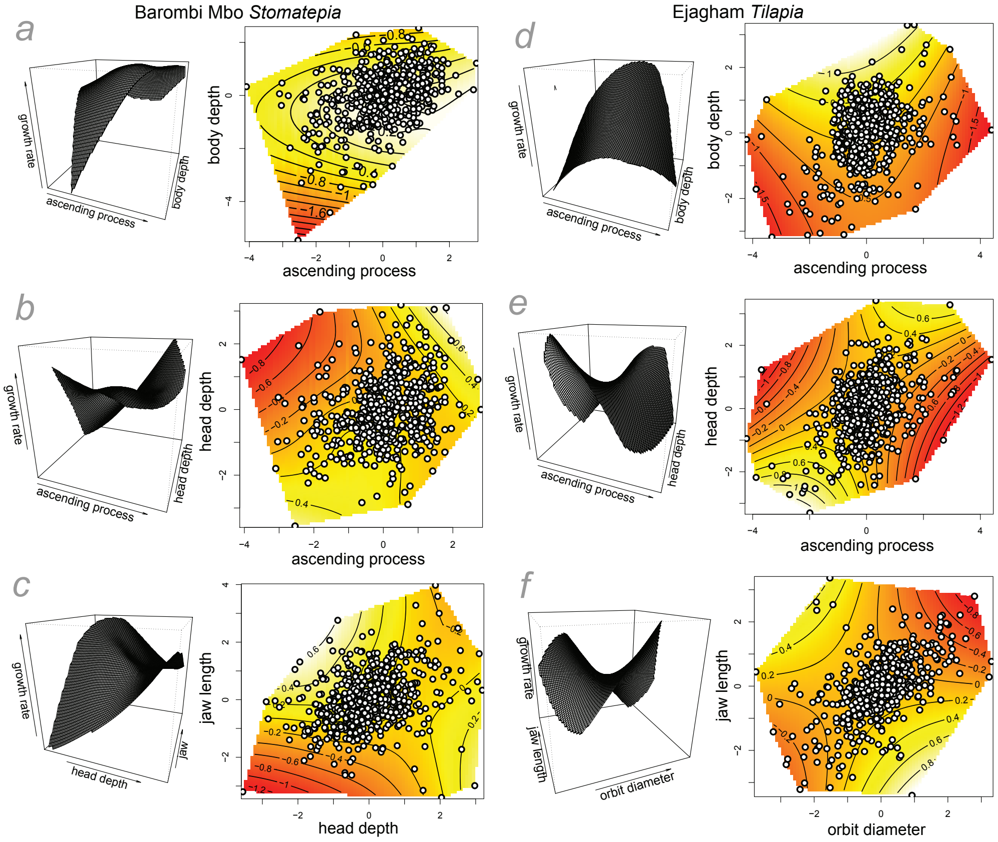

Figure 4: Perspective and contour plots illustrating major nonlinear selection surfaces in Barombi Mbo *Stomatepia* (*a-c*) and Ejagham *Tilapia* (*d-f*), visualized using thin-plate splines. The largest quadratic and correlational selection gradients (table 1) are depicted for each species complex. Individuals measured for each surface are indicated by open circles on the contour plots. All size-corrected trait axes and contour plot isoclines indicating relative growth rates are in units of standard deviation from the mean. Smoothing parameters were chosen by minimizing the generalized cross-validation score, resulting in 8.4 and 4.2 effective degrees of freedom per trait axis for the five traits measured in Barombi Mbo and Ejagham, respectively.

Discussion

In all models of sympatric speciation by natural selection, strong disruptive selection is necessary to initially drive the evolution of reproductive isolation between ecotypes within a panmictic population (Kirkpatrick and Ravigne 2002; Coyne and Orr 2004; Gavrilets 2004; Bolnick and Fitzpatrick 2007; Otto et al. 2008). As phenotypic divergence proceeds, the selection surface flattens, resulting in weak or absent disruptive selection after phenotypic separation is complete (Dieckmann and Doebeli 1999; Bolnick and Doebeli 2003). To test these predictions, empirical estimates of the current strength of disruptive selection are needed from the most plausible examples of sympatric speciation in nature. Ideally, these examples should also be in the earliest stages of divergence to best infer the initial conditions necessary for sympatric divergence.

I measured nonlinear and directional selection on functional traits within incipient species complexes from two of the most compelling cases of sympatric speciation, the Cameroon cichlids of crater lake Barombi Mbo and Lake Ejagham (Schliewen et al. 1994, 2001; Schliewen and Klee 2004). I found significant disruptive, stabilizing, correlational, and directional selection across several functional traits in each species complex using relative growth rates as a proxy for fitness (fig. 4; tables 1–3). However, the strength of disruptive selection was weaker than stabilizing and directional selection in both species complexes (tables 1–3) and the largest estimates of disruptive selection ob-

Table 2: **M** matrix of eigenvectors from the canonical rotation of γ

$\mathbf{m}_i$	λ_i	Body depth	Head depth	Jaw length	Ascending process	Orbit diameter
Lake Barombi Mbo *Stomatepia pindu/mariae*:						
$\mathbf{m}_1$	**.06**	−.11	−.88	.39	−.21	−.10
$\mathbf{m}_2$	*.03****	.01	.14	.68	.42	.59
$\mathbf{m}_3$	**.02**	−.07	−.003	.17	.70	−.69
$\mathbf{m}_4$	**−.10**	−.72	−.23	−.45	.36	.33
$\mathbf{m}_5$	**−.12**	−.68	.39	.39	−.41	−.25
Lake Ejagham: *Tilapia* (*Coptodon*) *deckerti/fusiforme/ejagham*:						
$\mathbf{m}_1$	*.12***	−.65	.68	−.07	.34	−.02
$\mathbf{m}_2$	**.11**	−.36	−.32	.68	.06	−.55
$\mathbf{m}_3$	*−.03*	.66	.41	.31	.49	−.24
$\mathbf{m}_4$	**−.05**	−.04	.03	.63	.02	.78
$\mathbf{m}_5$	*−.14*	−.11	−.52	−.22	.80	.18

Note: The eigenvalue (λ_i) of each eigenvector ($\mathbf{m}_i$) indicates the nonlinear selection gradient for each axis with all correlational selection removed. Correlation coefficients between each eigenvector and all traits measured are shown in each row. Boldface and italics indicate disruptive and stabilizing selection, respectively, along each multivariate axis as estimated in the full quadratic model.

** $P < .01$.

*** $P < .001$.

served in this study were not exceptional relative to published estimates of disruptive selection (fig. 5; Kingsolver et al. 2001*b*), falling within the range of single-species populations of lake stickleback that failed to speciate (Bolnick and Lau 2008; Bolnick 2011).

Weak or absent disruptive selection is predicted by theory after phenotypic separation has occurred (Doebeli and Dieckmann 1999). However, neither species complex displayed more than one mode along any trait axis (fig. 2), in contrast to many other examples of recent sympatric adaptive radiation (Hendry et al. 2009; Elmer et al. 2010; Martin and Wainwright 2011). Bayesian cluster analysis did support two clusters within each species complex; however, these clusters partially overlapped (figs. S2, S4, S6), and there was considerable uncertainty in assignment of individuals to each cluster. Major nonlinear surfaces within each lake were generally saddle shaped, and individuals clustered in the bowl of each saddle rather than dividing between distinct fitness peaks (fig. 4).

Trait unimodality was not due to overrepresentation of a single species in field samples. Unambiguous adults of multiple species in each species complex were frequently collected and exhibited the full phenotypic range described (Trewavas et al. 1972; Dunz and Schliewen 2010). Rather, there was a preponderance of individuals with intermediate morphologies that could not confidently be assigned to species by morphology alone. Ambiguity was also noted in the species descriptions of Ejagham *Tilapia*: species could be identified based only on adult breeding coloration, and morphometric analyses did not fully discriminate the four described *Tilapia* species (Dunz and Schliewen 2010; morphometric analyses have not been published previously for Barombi Mbo cichlids). Nonetheless, there is some evidence for significant population genetic structure among the nominal species within each species complex: two individuals each of *Stomatepia mariae*, *Stomatepia pindu*, and *Stomatepia mongo* were supported as monophyletic groups by AFLP analysis (Schliewen and Klee 2004; it is unknown whether these were random samples or targeted) and breeding adults from all four *Tilapia* species showed distinct population genetic structure based on microsatellite data with support for at least four genetic clusters within the *Tilapia* complex (Dunz and Schliewen 2010).

Overall, this suggests that these species complexes are still in the earliest stages of speciation, within the range where theory predicts that strong disruptive selection is necessary to complete sympatric speciation. Some flattening of the fitness surface within a diverging population occurs even before ecotype clusters split into distinct phenotypic modes (Dieckmann and Doebeli 1999); thus, the strength of disruptive selection within these species complexes is still predicted to be weaker than at the start of sympatric divergence. However, even doubling the estimate of the largest disruptive selection gradient ($2\gamma = 0.1$; table 1) still places these species complexes within only the top 33% of published estimates of disruptive selection ($n = 74/226$ estimates of positive quadratic selection gradients ≥ 0.2; Kingsolver et al. 2001*a*, 2001*b*), which were frequently severely underestimated (Blows and Brooks 2003; Stinchcombe et al. 2008). It is thus reasonable to conclude that the observed rates of disruptive selection are weaker than theory predicts is necessary to drive sym-

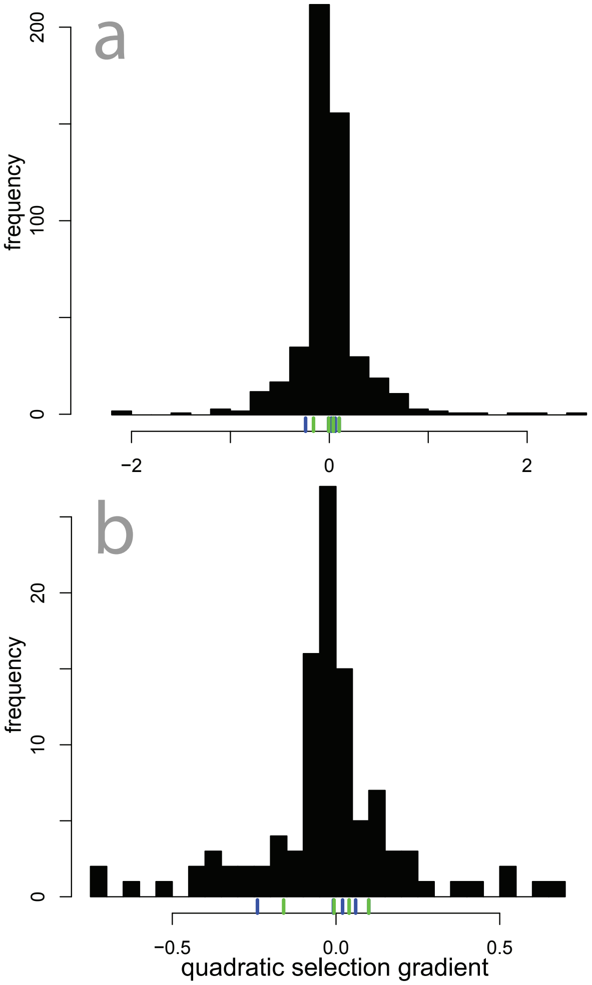

Figure 5: Standardized quadratic selection coefficients estimated for Barombi Mbo *Stomatepia* (blue lines) and Ejagham *Tilapia* (green lines; table 1) relative to the distribution of standardized quadratic selection coefficients estimated in the literature from 1984 to 1998 (Kingsolver et al. 2001*b*) in all taxa (*a*) and restricted to vertebrates (*b*).

patric speciation to completion (Dieckmann and Doebeli 1999; Matessi et al. 2001; Bolnick and Doebeli 2003). Nonetheless, relative growth rate is only one fitness component and additional ecological selection on survival and fecundity could ultimately result in greater curvature of the selection surface across total lifetime fitness. Furthermore, theoretical predictions depend on Gaussian assumptions for fitness curves (Baptestini et al. 2009; Thibert-Plant and Hendry 2009), whereas empirical fitness landscapes across an adaptive radiation may be much more complex (Schluter and Grant 1984; C. H. Martin and P. C. Wainwright, unpublished manuscript).

Despite morphological unimodality, individuals displayed bimodal species-diagnostic coloration that was weakly linked to divergent morphology in both species complexes (fig. 3) and linked to divergent dietary sources of benthic or limnetic carbon in Ejagham *Tilapia*. Eighty-six percent of Barombi Mbo *Stomatepia* could be assigned to either *S. mariae* or *S. pindu* coloration. Only breeding pairs of Ejagham *Tilapia* displayed species-diagnostic coloration, but 100% of collected breeding individuals in two species ($n = 50$) and pairs observed in the field (*Tilapia fusiforme*, $n = 31$; *Tilapia deckerti*, $n = 24$; *Tilapia ejagham*, $n = 2$) could be assigned to one of three species-diagnostic color categories. Coloration appears to be diverging more rapidly than trophic morphology and ecology in both species complexes and may suggest a more important role for sexual selection than ecological selection in driving initial sympatric diversification in these species complexes (similar to incipient species complexes of Malawi cichlids; Martin and Genner 2009).

Limited Progress toward Sympatric Speciation

These two sympatric species complexes appear to be in the initial stages of speciation in which a unimodal population experiences disruptive selection and shows signs of genetic structure and assortative mating between ecotypes but has not split into multiple phenotypic modes (Snowberg and Bolnick 2008; Bolnick 2011). Interestingly, phenotypic bimodality is often the criterion for successful sympatric speciation in theoretical models (Dieckmann and Doebeli 1999; Bolnick 2011), so in this sense these two "species" complexes have not speciated (alternatively, bimodal coloration could be considered sympatric speciation by sexual selection). Theoretical models also indicate that incomplete sympatric speciation can be an equilibrium state that will never progress to complete phenotypic separation if either the strength of selection or assortative mating is weak, the costs of female choosiness are high, or numerous loci underlie ecological traits (Matessi et al. 2001; Bolnick 2004*b*, 2006). In contrast, many species may also arise simultaneously during sympatric divergence if individual niche widths are sufficiently narrow relative to the resource distribution (Bolnick 2006). Thus, ecologically driven sympatric speciation in these cichlid adaptive radiations may have occurred in a simultaneous burst, resulting in daughter species that exceeded the boundaries of one or more parameter ranges necessary for sympatric divergence to proceed to completion and became stalled in a permanent state of incomplete phenotypic and ecological divergence.

In contrast, species-diagnostic coloration in both species complexes showed the most pronounced divergence out of all traits and trophic axes examined. This contradicts conventional wisdom that ecological selection mediated by competition for resources among ecotypes is the pri-

Table 3: Alignment of the phenotypic variance-covariance matrix (**P**) with the nonlinear selection surface (**M**; see table 2)

Vectors	PC1	PC2	PC3
Lake Barombi Mbo *Stomatepia pindu*/*mariae*:			
Parallel	*.02–.20*	*.04–.23*	*.05–.34*
$\mathbf{m}_1$	.90–.94	.97–.99	.58–.85
$\mathbf{m}_2$	.56–.77	.71–.91	.91–.97
$\mathbf{m}_3$	.92–.99	.74–.86	.85–.99
$\mathbf{m}_4$	.88–.94	.90–.97	.86–.99
$\mathbf{m}_5$	.97–.99	.85–.94	.84–.98
Lake Ejagham: *Tilapia* (*Coptodon*) *deckerti*/*fusiforme*/*ejagham*:			
Parallel	*.01–.08*	*.04–.23*	*.08–.82*
$\mathbf{m}_1$	.99–.99	.96–.99	.22–.96
$\mathbf{m}_2$	.95–.97	.91–.97	.90–.99
$\mathbf{m}_3$	.51–.58	.92–.97	.95–.99
$\mathbf{m}_4$	.87–.91	.52–.68	.91–.99
$\mathbf{m}_5$	.99–.99	.88–.98	.49–.99

Note: The first three principal components of **P**, PC1–PC3 (columns), were compared with the five eigenvectors from the canonical rotation of γ, $\mathbf{m}_{1-5}$ (rows) for each species complex. Empirical 95% confidence intervals are shown for the distribution of the sin of the angle (sin θ) between each pair of vectors, where a value of 1 indicates orthogonal vectors and 0 indicates parallel vectors. Distributions of sin θ were generated by bootstrapping **P** with replacement and recalculating PC1–PC3 in each bootstrap sample. The expected 95% confidence intervals for parallel vectors are also shown for PC1–PC3, estimated from the distribution of sin θ between each observed vector and bootstrapped samples from that vector.

mary and initial driver of sympatric speciation and adaptive radiation, a model that has often been proposed for African cichlids in particular (Schliewen et al. 1994; Streelman and Danley 2004). Instead, disruptive sexual selection on coloration within each species complex may be the primary driver of initial reproductive isolation, preceding substantial morphological or ecological divergence, as observed in both species complexes. Alternatively, lineage-through-time plots suggest that the Barombi Mbo cichlid radiation went through two bursts of speciation, interrupted by a period of stasis, over approximately 1 million years (Seehausen 2006). This first burst may have corresponded to primarily ecologically driven speciation and the evolution of all trophic specializations within the lake, followed by primarily sexually driven, incomplete speciation forming species complexes in the second burst, similar to the model of Streelman and Danley (2004). Finally, increased introgression due to anthropogenic disturbances (see below) cannot be ruled out and may have resulted in increased abundance of morphological intermediates (e.g., due to relaxed postzygotic extrinsic isolation) while disruptive sexual selection driving bimodal coloration remained intact.

Additional Constraints on Phenotypic Divergence

Beyond weak disruptive selection, what other factors may have slowed or halted phenotypic divergence in these species complexes? One likely constraint is fluctuation in the stability and strength of disruptive selection through time (Grant and Grant 2002). Field samples were collected near the end of the dry season, when resources were likely limited due to reduced allochthonous material, thus disruptive selection may be weaker or even reverse direction at other times of year. Sampling also occurred in one of the hottest years on record near the beginning of a major El Niño–Southern Oscillation event that included many global climate anomalies (Seager et al. 2010), suggesting this sample could represent an outstanding year for resource limitation.

Second, stabilizing, correlational, and directional selection gradients were stronger than disruptive selection on any single trait in both lakes (table 1). This may constrain phenotypic divergence due to pleiotropy between traits experiencing stabilizing and disruptive selection or limited phenotypic variation along higher-dimensional trait axes (Kirkpatrick 2010). Third, in contrast to other studies of speciation (Schluter 1996; Blows et al. 2004), the major axes of the phenotypic variance-covariance matrix (**P**) were not aligned with the major axes of the nonlinear selection surface in either species complex (table 3). Matrix **P** provides an estimate of the genetic variance-covariance matrix (**G**), which can constrain both the rate and direction of trait evolution if limited genetic variance reduces evolvability in certain trait dimensions (Schluter 1996; Blows et al. 2004;

Mezey and Houle 2005). The three largest eigenvectors of **P** were not aligned with any of the five largest nonlinear selection axes (including both stabilizing and disruptive selection; tables 2, 3), suggesting either fluctuating nonlinear selection or some phenotypic constraint.

Alternatively, human disturbance in both lakes may have resulted in the recent collapse of bimodality, as suggested for some populations of Darwin's finches (De Leon et al. 2011) and other lacustrine fish radiations (Seehausen et al. 1997; Strecker 2006; Vonlanthen et al. 2012). In 2000–2001, a population of the predatory catfish *Parauchenoglanis* cf. *balayi*, reaching 40 cm, was intentionally introduced to Lake Ejagham from the neighboring river by a member of the town council and was frequently captured in gill nets during field sampling. It is unknown what impacts this species is having on the endemic fauna, but all species from this tiny 0.5-km^2 lake should now be considered critically endangered. No invasive fish species have been introduced to Barombi Mbo, but slash-and-burn agriculture inside the entire crater rim (C. H. Martin, personal observation) may have altered the environment through increased silt and nutrient inputs. Nonetheless, species complexes in both lakes experienced disruptive selection at the time of sampling even within these disturbed environments. Although future impacts on the selection environment are likely, particularly within Lake Ejagham, current measurements of selection in these lakes still represent the best available estimates of selection during the initial stages of sympatric speciation in these radiations.

Is Sympatric Speciation Slow?

Is slow phenotypic divergence within these two species complexes a symptom of speciation under fully sympatric conditions? Both allopatric speciation and speciation with gene flow can occur rapidly when driven by divergent natural selection (Hendry and Kinneson 1999), but sympatric speciation is traditionally thought to be fastest (McCune and Lovejoy 1998). However, models of sympatric speciation frequently suggest long waiting times for speciation, particularly if parameter ranges are suboptimal (Bolnick 2004*b*) or in the absence of "magic" traits that both experience disruptive selection and cause assortative mating (Dieckmann and Doebeli 1999). Alternatively, incomplete sympatric speciation is often an evolutionary stable state in these models (Matessi et al. 2001; Bolnick 2004*b*, 2006). Estimates of disruptive selection in this study did not stand out among a broad survey of quadratic selection gradients in the literature (fig. 5; Kingsolver et al. 2001*b*), many of which were probably underestimated due to lack of canonical rotation (Blows et al. 2004) or failure to double quadratic parameters from statistical models (Stinchcombe et al. 2008). Furthermore, strong linkage disequilibrium between morphological ecotype and species-diagnostic coloration was lacking in both species complexes (fig. 3), demonstrating the absence of a pleiotropic magic trait (Servedio et al. 2011). If coloration provides the major mate choice cue for assortative mating in *Stomatepia*, this observation suggests that magic traits did not initially facilitate sympatric speciation in these species complexes, in contrast to many other examples of sympatric divergence (Sorenson et al. 2003; Seehausen et al. 2008; Papadopulos et al. 2011). However, many additional mate cues can be involved in cichlid mate choice, such as behavioral displays, sound production, olfactory cues, and territory (Candolin 2003), including UV reflectance and UV opsin sensitivity in Barombi Mbo cichlids (Timelthaler 2010), providing ample opportunities for direct or indirect divergent ecological selection on these assortative mating traits. Furthermore, the costs of assessing multiple males for multiple cues may be incredibly low; for example, Lake Malawi *Nyassachromis microcephalus* cichlid females assessed up to 135 courting males during a single hour-long visit to the lek (Martin 2010).

However, long waiting times for sympatric speciation in Barombi Mbo *Stomatepia* and Ejagham *Tilapia* do not explain the complete phenotypic separation of other cichlid species within each sympatric lake radiation. For example, within the Barombi Mbo species flock, individuals from the four-species *Sarotherodon* complex were also difficult to assign to species, whereas the monotypic species *Myaka myaka* and *Pungu maclareni* were highly morphologically distinct (C. H. Martin, personal observation; Trewavas et al. 1972). In Lake Ejagham, the sister species *Sarotherodon lamprechti* and *Sarotherodon knauerae* were readily distinguished in the field (C. H. Martin, personal observation) and showed nonoverlapping clusters in morphospace (Neumann et al. 2011). This suggests a complex pattern of progress toward speciation not just between lakes but between the two independent cichlid invasions of Lake Ejagham (*Sarotherodon* and *Tilapia* lineages) and among different clades within the Barombi Mbo cichlid radiation. Moreover, *Clarias* catfishes may have also speciated within Barombi Mbo, while several other lineages of fishes (*Aphyosemion*, *Procatopus*, *Barbus*) have failed to speciate in both Ejagham and Barombi Mbo (Trewavas et al. 1972; Schliewen et al. 2001).

In contrast to the species complexes studied here, why are Barombi Mbo *Myaka* and *Pungu* and Ejagham *Sarotherodon* species morphologically separated (i.e., each species occupies distinct phenotypic modes)? One possibility is that speciation in these taxa may have occurred through different mechanisms. *Myaka myaka* is nested within the Barombi Mbo *Sarotherodon* clade (Schliewen and Klee 2004), but adults are found exclusively offshore in the pelagic zone, suggesting parapatric speciation or that divergent habitat preferences automatically generated assortative mating in *Myaka* (i.e., the presence of a magic trait). Similarly, only one of the two *Sarotherodon* species in Lake Ejagham was frequently encountered in the littoral zone, while the other species was only captured in deeper gill nets, suggesting that habitat preferences may have contributed to reproductive isolation in this species pair unlike the two species complexes studied here that occupied overlapping habitats. Finally, *Pungu maclareni* may be a hybrid species resulting from interbreeding of the *Konia* and *Sarotherodon* lineages in Barombi Mbo (Schliewen and Klee 2004).

Second, the morphologically distinct species within each lake also occupy highly divergent ecological niches in contrast to the species complexes studied here. For example, *Myaka myaka* is the only zooplanktivore in Barombi Mbo, *Pungu maclareni* is a specialized spongivore, and *Sarotherodon lamprechti* is reported to be the only phytoplanktivore in Ejagham (Neumann et al. 2011). In contrast, the Barombi Mbo *Stomatepia* species studied here are both insectivores and the Ejagham *Tilapia* are omnivores (Trewavas et al. 1972; Dunz and Schliewen 2010) with very little separation in limnetic-benthic carbon sources as indicated by stable isotope signatures in two of these species (mean $\delta^{13}C : -29.5$ vs. -28.4). Consistent with this view, the dietary divergence in limnetic-benthic carbon sources and trophic position of *Pungu maclareni* from *Stomatepia* was 5.6 and 2.3 times greater than dietary divergence between the two nominal species of *Stomatepia*. Thus, increased trophic specialization in the ecologically novel Cameroon cichlid species may be driving rapid morphological diversification, as observed in two incipient adaptive radiations of *Cyprinodon* pupfishes in which unique trophic specialist species diverged up to 130 times faster for certain trophic traits than in other pupfish clades, even clades of similar age adapting to similar novel environments (Martin and Wainwright 2011). Adapting to novel ecological niches, such as sponge eating, may require a greater magnitude of phenotypic divergence along a larger number of trait axes, driving increased phenotypic separation in these species (Martin and Wainwright 2011; also see Nosil et al. 2008).

Conclusion

One species complex within each of two radiations of Cameroon cichlids has not diverged into bimodal morphological clusters (fig. 2), despite significant disruptive selection (fig. 4), morphologically divergent species coloration (fig. 3), and genetic differentiation among species (Schliewen and Klee 2004; Dunz and Schliewen 2010). In contrast to previous work highlighting ecological speciation as complete in these radiations, I found these species complexes to be in the very early stages of divergence with more pronounced differences in sexual coloration than trophic morphology or diet, consistent with a more important role for sexual selection than natural selection in the early stages of sympatric speciation and adaptive radiation (contra Streelman and Danley 2004).

There are several non-mutually exclusive explanations for incomplete phenotypic divergence. (1) Sympatric speciation is slow or incomplete due to weak disruptive selection and/or the lack of magic traits in these species complexes. The strength of standardized disruptive selection gradients was not large relative to published estimates (fig. 5). In Barombi Mbo *Stomatepia*, species-diagnostic coloration was not tightly linked to species-diagnostic morphology, indicating the absence of pleiotropy between this assortative mating cue and traits under divergent selection. (2) Sympatric speciation is constrained by stabilizing and directional selection on other trait axes (tables 1, 2), lack of alignment between major phenotypic axes of variance and major axes of nonlinear selection (table 3), or fluctuating nonlinear selection regimes. (3) Alternatively, the ecological similarity of ecotypes within each species complex may constrain their phenotypic divergence in contrast to the morphologically distinct and trophically specialized species within each radiation (also see Martin and Wainwright 2011). (4) Finally, I cannot rule out that bimodality, and possibly strong disruptive selection, may have recently collapsed in both species complexes due to increasing anthropogenic disturbances. Overall, this work provides a starting point in two of our most compelling examples of sympatric speciation in nature for identifying and measuring the conditions that may be essential for this process.

Acknowledgments

Funding was provided by a Young Explorer's Grant from the National Geographic Society, the Lewis and Clark Fund from the American Philosophical Society, a National Science Foundation Graduate Research Fellowship, and the Center for Population Biology. C. Dening provided invaluable logistical field support; P. Enyong supported fieldwork at Lake Ejagham; N. Gonwuou assisted with obtaining permits; and S. Romero, A. Tan, C. Norton, B. Breen, and R. Koch assisted with processing, photographing, and measuring scales and specimens. D. Bolnick, S. Price, and two anonymous reviewers provided comments on the manuscript, and M. Turelli, P. Wainwright, and the Wainwright lab group provided helpful discussion of the project. I also graciously thank Pa'a Chief of Barombi Mbo village; Chief Obi of Eyumojock village; and the Ministry of Scientific Research and Innovation, Republic of Cameroon, for permission to conduct this research.

Literature Cited

Albertson, R. C., J. T. Streelman, and T. D. Kocher. 2003. Directional selection has shaped the oral jaws of Lake Malawi cichlid fishes. Proceedings of the National Academy of Sciences of the USA 100: 5252–5257.

Arnold, S. J., R. Burger, P. A. Hohenlohe, B. C. Ajie, and A. G. Jones. 2008. Understanding the evolution and stability of the G-matrix. Evolution 62:2451–2461.

Arnold, S. J., M. E. Pfrender, and A. G. Jones. 2001. The adaptive landscape as a conceptual bridge between micro- and macroevolution. Genetica 112–113:9–32.

Baptestini, E. M., M. A. de Aguiar, D. I. Bolnick, and M. S. Araújo. 2009. The shape of the competition and carrying capacity kernels affects the likelihood of disruptive selection. Journal of Theoretical Biology 259:5–11.

Barlow, C. G., and B. A. Gregg. 1991. Use of circuli spacing on scales to discriminate hatchery and wild barramundi, *Lates calcarifer* (Bloch). Aquaculture and Fisheries Management 22:491–498.

Barluenga, M. K., and A. Meyer. 2010. Phylogeography, colonization and population history of the Midas cichlid species complex (*Amphilophus* spp.) in the Nicaraguan crater lakes. BMC Evolutionary Biology 10:326.

Barluenga, M., K. N. Stolting, W. Salzburger, M. Muschick, and A. Meyer. 2006. Sympatric speciation in Nicaraguan crater lake cichlid fish. Nature 439:719–723.

Bates, D. 2006. [R] lmer, p-values, and all that. R-help mailing list. https://stat.ethz.ch/pipermail/r-help/2006-May/094765.html.

Bates, D., M. Maechler, and B. Bolker. 2012. lme4: linear mixed-effects models using S4 classes. R package version 0.999375–33. http://cran.r-project.org/package = lme4.

Berlocher, S. H., and J. L. Feder. 2002. Sympatric speciation in phytophagous insects: moving beyond controversy? Annual Review of Entomology 47:773–813.

Bilton, H. T. 1975. Factors influencing the formation of scale characters. International North Pacific Fisheries Community Bulletin 32:102–108.

Blows, M. W. and R. Brooks. 2003. Measuring nonlinear selection. American Naturalist 162:815–820.

Blows, M. W., S. F. Chenoweth, and E. Hine. 2004. Orientation of the genetic variance-covariance matrix and the fitness surface for multiple male sexually selected traits. American Naturalist 163:329–340.

Blows, M. W., and M. Higgie. 2003. Genetic constraints on the evolution of mate recognition under natural selection. American Naturalist 161:240–253.

Bolnick, D. I. 2004*a*. Can intraspecific competition drive disruptive selection? an experimental test in natural populations of stickleback. Evolution 58:608–618.

———. 2004*b*. Waiting for sympatric speciation. Evolution 58:895–899.

———. 2006. Multi-species outcomes in a common model of sympatric speciation. Journal of Theoretical Biology 214:734–744.

———. 2011. Sympatric speciation in threespine stickleback: why not? International Journal of Ecology 2011:1–14.

Bolnick, D. I., and M. Doebeli. 2003. Sexual dimorphism and adaptive speciation: two sides of the same ecological coin. Evolution 57:2433–2449.

Bolnick, D. I., and B. M. Fitzpatrick. 2007. Sympatric speciation: models and empirical evidence. Annual Review of Ecology and Systematics 38:459–487.

Bolnick, D. I., and O. L. Lau. 2008. Predictable patterns of disruptive selection in stickleback in postglacial lakes. American Naturalist 172:1–11.

Buckley, L. J. 1984. RNA-DNA ratio: an index of larval fish growth in the sea. Marine Biology 80:291–298.

Candolin, U. 2003. The use of multiple cues in mate choice. Biological Reviews 78:575–595.

Cheung, C. H. Y., P. M. Chaillé, D. J. Randall, J. S. Gray, and D. W. T. Au. 2007. The use of scale increment as a means of indicating fish growth and growth impairment. Aquaculture 266:102–111.

Cheverud, J. M. 1988. A comparison of genetic and phenotypic correlations. Evolution 42:958–968.

Connell, J. H. 1980. Diversity and the coevolution of competitors, or the ghost of competition past. Oikos 35:131–138.

Cornen, G., Y. Bandet, P. Giresse, and J. Maley. 1992. The nature and chronostratigraphy of Quaternary pyroclastic accumulations from Lake Barombi Mbo (West-Cameroon). Journal of Volcanology and Geothermal Research 51:357–374.

Coyne, J. A., and H. A. Orr. 2004. Speciation. Sinauer, Sunderland, MA.

Darwin, C. 1859. On the origin of species by means of natural selection. J. Murray, London.

De Leon, L. F., J. A. Raeymaekers, E. Bermingham, J. Podos, A. Herrel, and A. P. Hendry. 2011. Exploring possible human influences on the evolution of Darwin's finches. Evolution 65:2258–2272.

Dieckmann, U., and M. Doebeli. 1999. On the origin of species by sympatric speciation. Nature 400:354–357.

Doebeli, M., U. Dieckmann, J. A. J. Metz, and D. Tautz. 2005. What we have also learned: adaptive speciation is theoretically plausible. Evolution 59:691–695.

Doroszuk, A., M. W. Wojewodzic, G. Gort, and J. E. Kammenga. 2008. Rapid divergence of genetic variance-covariance matrix within a natural population. American Naturalist 171:291–304.

Doyle, R. W., A. J. Talbot, and R. R. Nicholas. 1987. Statistical interrelation of length, growth, and scale circulus spacing: appraisal of a growth rate estimator for fish. Canadian Journal of Fisheries and Aquatic Sciences 44:1520–1528.

Dunz, A. R., and U. K. Schliewen. 2010. Description of a *Tilapia* (*Coptodon*) species flock of Lake Ejagham (Cameroon), including a redescription of *Tilapia deckerti* Thys van den Audenaerde, 1967. Spixiana 33:251–280.

Elmer, K. R., T. K. Lehtonen, A. F. Kautt, C. Harrod, and A. Meyer. 2010. Rapid sympatric ecological differentiation of crater lake cichlid fishes within historic times. BMC Biology 8:60.

Felsenstein, J. 1981. Skepticism towards Santa Rosalia, or why are there so few kinds of animals? Evolution 35:124–138.

Fields Development Team. 2006. Fields: tools for spatial data. National Center for Atmospheric Research, Boulder, CO. http://www.image.ucar.edu/Software/Fields/.

Fisher, J. P., and W. G. Pearcy. 1990. Spacing of scale circuli versus growth rate in young coho salmon. Fisheries Bulletin 88:637–643.

———. 2005. Seasonal changes in growth of coho salmon (*Oncorhynchus kisutch*) off Oregon and Washington and concurrent changes in the spacing of scale circuli. Fisheries Bulletin 2005:34–51.

Fitzpatrick, B. M., J. A. Fordyce, and S. Gavrilets. 2008. What, if anything, is sympatric speciation? Journal of Evolutionary Biology 21:1452–1459.

Flint-Garcia, S. A., J. M. Thornsberry, and E. S. T. Buckler. 2003.

Structure of linkage disequilibrium in plants. Annual Review of Plant Biology 54:357–374.

Fraley, C. F., and A. E. Raftery. 2007. Model-based methods of classification: using the mclust software in chemometrics. Journal of Statistical Software 18:1–13.

Fukuwaka, M., and M. Kaeriyama. 1997. Scale analyses to estimate somatic growth in sockeye salmon, *Oncorhynchus nerka*. Canadian Journal of Fisheries and Aquatic Sciences 54:631–636.

Gavrilets, S. 2004. Fitness landscapes and the origin of species. Princeton University Press, Princeton, NJ.

Gavrilets, S., A. Vose, M. Barluenga, W. Salzburger, and A. Meyer. 2007. Case studies and mathematical models of ecological speciation. 1. Cichlids in a crater lake. Molecular Ecology 16:2893–2909.

Grant, P. R., and B. R. Grant. 2002. Unpredictable evolution in a 30-year study of Darwin's finches. Science 296:707–711.

Green, J. 1972. Ecological studies on crater lakes in West Cameroon zooplankton of Barombi Mbo, Mboandong, Lake Kotto and Lake Soden. Journal of Zoology 166:283–301.

Hansen, T. F., and D. Houle. 2008. Measuring and comparing evolvability and constraint in multivariate characters. Journal of Evolutionary Biology 21:1201–1219.

Hartigan, J. A., and P. M. Hartigan. 1985. The dip test of unimodality. Annals of Statistics 13:70–84.

Healey, M. C. 1982. Timing and relative intensity of size-selective mortality of juvenile chum salmon (*Oncorhynchus keta*) during early sea life. Canadian Journal of Fisheries and Aquatic Sciences 39:952–957.

Hendry, A. P., S. K. Huber, L. F. De Leon, A. Herrel, and J. Podos. 2009. Disruptive selection in a bimodal population of Darwin's finches. Proceedings of the Royal Society B: Biological Sciences 276:753–759.

Hendry, A. P., and M. T. Kinnison. 1999. Perspective: the pace of modern life: measuring rates of contemporary evolution. Evolution 53:1637–1653.

Hubley, P. B., P. G. Amiro, and A. J. F. Gibson. 2008. Changes in scale circulus spacings of an endangered Atlantic salmon *Salmo salar* population: evidence of a shift in marine migration? Journal of Fish Biology 73:2321–2340.

Ibáñez, A. L., J. R. Britton, and I. G. Cowx. 2008. Relationship between scale growth checks, circuli formation rate and somatic growth in *Rutilus rutilus* (L.) a fish farm-reared cyprinid. Journal of Fish Biology 72:1023–1034.

Kingsford, M. J., and M. H. Atkinson. 1994. Increments in otoliths and scales: how they relate to the age and early development of reared and wild larval and juvenile *Chrysophrys auratus*. Australian Journal of Marine and Freshwater Research 45:1007–1021.

Kingsolver, J. G., H. E. Hoekstra, J. M. Hoekstra, D. Berrigan, S. N. Vignieri, C. E. Hill, A. Hoang, P. Gilbert, and P. Beerli. 2001*a*. The strength of phenotypic selection in natural populations. American Naturalist 157:245–261.

———. 2001*b*. Data from: The strength of phenotypic selection in natural populations. American Naturalist 157:245–261. Dryad digital repository, doi:10.5061/dryad.166.

Kingsolver, J. G., and D. W. Pfennig. 2007. Patterns and power of phenotypic selection in nature. BioScience 57:561–572.

Kirkpatrick, M. 2010. Limits on rates of adaptation: why is Darwin's machine so slow? *In* M. A. Bell, D. J. Futuyma, W. F. Eanes, and J. S. Levinton, eds. Evolution since Darwin: the first 150 years. Sinauer, Sunderland, MA.

Kirkpatrick, M., and N. Barton. 2006. Chromosome inversions, local adaptation and speciation. Genetics 173:419–434.

Kirkpatrick, M., and V. Ravigne. 2002. Speciation by natural and sexual selection: models and experiments. American Naturalist 159:S22–S35.

Kisel, Y., and T. G. Barraclough. 2010. Speciation has a spatial scale that depends on levels of gene flow. American Naturalist 175:316–334.

Kling, G. W. 1988. Comparative transparency, depth of mixing, and stability of stratification in lakes of Cameroon, West Africa. Limnology and Oceanography 33:27–40.

Kobayashi, T. 1961. Biology of chum salmon, *Oncorhynchus keta* (Walbaum), by the growth formula of scales. Science Reports of the Hokkaido Salmon Hatchery 16:1–102.

Kocher, T. D. 2004. Adaptive evolution and explosive speciation: the cichlid fish model. Nature Reviews Genetics 5:288–298.

Kolbe, J. J., L. J. Revell, B. Szekely, E. D. Brodie, and J. B. Losos. 2011. Convergent evolution of phenotypic integration and its alignment with morphological diversification in Caribbean *Anolis* ecomorphs. Evolution 65:3608–3624.

Kondrashov, A. S., and F. A. Kondrashov. 1999. Interactions among quantitative traits in the course of sympatric speciation. 400:351–354.

Lande, R. 1979. Quantitative genetic analysis of multivariate evolution, applied to brain : body size allometry. Evolution 33:402–416.

Lande, R., and S. J. Arnold. 1983. The measurement of selection on correlated characters. Evolution 37:1210–1226.

Lenth, R. V. 2009. Response-surface methods in R, using rsm. Journal of Statistical Software 32:2–17.

Maan, M. E., and O. Seehausen. 2011. Ecology, sexual selection and speciation. Ecology Letters 14:591–602.

Mallet, J., A. Meyer, P. Nosil, and J. L. Feder. 2009. Space, sympatry, and speciation. Journal of Evolutionary Biology 22:2332–2341.

Martin, C. H. 2010. Unexploited females and unreliable signals of male quality in a Malawi cichlid bower polymorphism. Behavioral Ecology 21:1195–1202.

Martin, C. H., and M. J. Genner. 2009. High niche overlap between two successfully coexisting pairs of Lake Malawi cichlid fishes. Canadian Journal of Fisheries and Aquatic Sciences 66:579–588.

Martin, C. H., and P. C. Wainwright. 2011. Trophic novelty is linked to exceptional rates of morphological diversification in two adaptive radiations of *Cyprinodon* pupfishes. Evolution 65:2197–2212.

Martin, R. A., and D. W. Pfennig. 2009. Disruptive selection in natural populations: the roles of ecological specialization and resource competition. American Naturalist 174:268–281.

Matessi, C., A. Gimelfarb, and S. Gavrilets. 2001. Long-term buildup of reproductive isolation promoted by disruptive selection: how far does it go? Selection 2:41–64.

McCune, A. R., and N. R. Lovejoy. 1998. The relative rate of sympatric and allopatric speciation in fishes: tests using DNA sequence divergence between sister species and among clades. *In* D. J. Howard and S. H. Berlocher, eds. Endless forms: species and speciation. Oxford University Press, Oxford.

Mezey, J. G., and D. Houle. 2005. The dimensionality of genetic variation for wing shape in *Drosophila melanogaster*. Evolution 59:1027–1038.

Michel, A. P., S. Sim, T. H. Q. Powell, M. S. Taylor, P. Nosil, and J. L. Feder. 2010. Widespread genomic divergence during sympatric speciation. Proceedings of the National Academy of Sciences of the USA 107:9724–9729.

Motta, P. J. 1984. Mechanics and functions of jaw protrusion in teleost fishes: a review. Copeia 1984:1–18.

Neumann, D., M. L. J. Stiassny, and U. K. Schliewen. 2011. Two new sympatric *Sarotherodon* species (Pisces: Cichlidae) endemic to Lake Ejagham, Cameroon, west-central Africa, with comments on the *Sarotherodon galilaeus* species complex. Zootaxa 2785:1–20.

Nosil, P., L. J. Harmon, and O. Seehausen. 2008. Ecological explanations for (incomplete) speciation. Trends in Ecology & Evolution 24:154–156.

Otto, S. P., M. R. Servedio, and S. L. Nuismer. 2008. Frequency-dependent selection and the evolution of assortative mating. Genetics 179:2091–2112.

Papadopulos, A. S. T., W. J. Baker, D. Crayn, R. K. Butlin, R. G. Kynast, I. Hutton, and V. Savolainen. 2011. Speciation with gene flow on Lord Howe Island. Proceedings of the National Academy of Sciences of the USA 108:13188–13193.

Pfennig, D. W., and K. S. Pfennig. 2010. Character displacement and the origins of diversity. American Naturalist 176(suppl.):S26–S44.

Phillips, P. C., and S. J. Arnold. 1989. Visualizing multivariate selection. Evolution 43:1209–1222.

Post, D. M. 2002. Using stable isotopes to estimate trophic position: models, methods, and assumptions. Ecology 83:703–718.

R Development Core Team. 2011. R: a language and environment for statistical computing. R Foundation for Statistical Computing, Vienna, Austria. http://www.r-project.org/.

Ripa, J. 2008. When is sympatric speciation truly adaptive? an analysis of the joint evolution of resource utilization and assortative mating. Evolutionary Ecology 23:31–52.

Roughgarden, J. 1972. Evolution of niche width. American Naturalist 106:683–718.

Schliewen, U. K., and B. Klee. 2004. Reticulate sympatric speciation in Cameroonian crater lake cichlids. Frontiers in Zoology 1:5.

Schliewen, U. K., T. D. Kocher, K. R. McKaye, O. Seehausen, and D. Tautz. 2006. Evolutionary biology: evidence for sympatric speciation? Nature 444:E12–E13.

Schliewen, U. K., K. Rassmann, M. Markmann, J. Markert, T. Kocher, and D. Tautz. 2001. Genetic and ecological divergence of a monophyletic cichlid species pair under fully sympatric conditions in Lake Ejagham, Cameroon. Molecular Ecology 10:1471–1488.

Schliewen, U. K., D. Tautz, and S. Paabo. 1994. Sympatric speciation suggested by monophyly of crater lake cichlids. Nature 368:629–632.

Schluter, D. 1996. Adaptive radiation along genetic lines of least resistance. Evolution 50:1766-1774.

Schluter, D., and P. R. Grant. 1984. Determinants of morphological patterns in communities of Darwin's finches. American Naturalist 123:175–196.

Schluter, D., and D. Nychka. 1994. Exploring fitness surfaces. American Naturalist 143:597–616.

Schwarz, G. 1978. Estimating the dimension of a model. Annals of Statistics 6:461–464.

Seager, R., Y. Kushnir, J. Nakamura, M. Ting, and N. Naik. 2010. Northern hemisphere winter snow anomalies: ENSO, NAO and the winter of 2009/10. Geophysical Research Letters 37:L14703.

Seehausen, O. 2006. African cichlid fish: a model system in adaptive radiation research. Proceedings of the Royal Society B: Biological Sciences 273:1987–1998.

Seehausen, O., Y. Terai, I. S. Magalhaes, K. L. Carleton, H. D. J. Mrosso, R. Miyagi, I. van der Sluijs, et al. 2008. Speciation through sensory drive in cichlid fish. Nature 455:620–626.

Seehausen, O., J. J. M. van Alphen, and F. Witte. 1997. Cichlid fish diversity threatened by eutrophication that curbs sexual selection. Science. 277:1808–1811.

Servedio, M. R., G. S. Van Doorn, M. Kopp, A. M. Frame, and P. Nosil. 2011. Magic traits in speciation: "magic" but not rare? Trends in Ecology & Evolution 26:389–397.

Simms, E. L., and M. D. Rausher. 1993. Patterns of selection on phytophage resistance in *Ipomoea purpurea*. Evolution 47:970–976.

Sire, J. Y. 1986. Ontogenetic development of surface ornamentation in the scales of *Hemichromis bimaculatus* (Cichlidae). Journal of Fish Biology 28:713–724.

Sire, J. Y., and I. Arnulf. 2000. Structure and development of the ctenial spines on the scales of a teleost fish, the cichlid *Cichlasoma nigrofasciatum*. Acta Zoologica 81:139–158.

Snowberg, L. K., and D. I. Bolnick. 2008. Assortative mating by diet in a phenotypically unimodal but ecologically variable population of stickleback. American Naturalist 172:733–739.

Sorenson, M. D., K. M. Sefc, and R. B. Payne. 2003. Speciation by host switch in brood parasitic indigobirds. Nature 424:928–931.

Steppan, S. J., P. C. Phillips, and D. Houle. 2002. Comparative quantitative genetics: evolution of the G matrix. Trends in Ecology & Evolution 17:320–327.

Stiassny, M. L. J., U. K. Schliewen, and W. J. Dominey. 1992. A new species flock of cichlid fishes from Lake Bermin, Cameroon with a description of eight new species of *Tilapia* (Labroidei: Cichlidae). Ichthyological Exploration of Freshwaters 3:311–346.

Stinchcombe, J. R., A. F. Agrawal, P. A. Hohenlohe, S. J. Arnold, and M. W. Blows. 2008. Estimating nonlinear selection gradients using quadratic regression coefficients: double or nothing? Evolution 62:2435–2440.

Strecker, U. 2006. The impact of invasive fish on an endemic *Cyprinodon* species flock (Teleostei) from Laguna Chichancanab, Yucatan, Mexico. Ecology of Freshwater Fish 15:408–418.

Streelman, J. T., and P. D. Danley. 2003. The stages of vertebrate evolutionary radiation. Trends in Ecology and Evolution 18:126–131.

Svänback, R., and D. I. Bolnick. 2007. Intraspecific competition drives increased resource use diversity within a natural population. Proceedings of the Royal Society B: Biological Sciences 274:839–844.

Swanson, B. O., A. C. Gibb, J. C. Marks, and D. A. Hendrickson. 2003. Trophic polymorphism and behavioral differences decrease intraspecific competition in a cichlid, *Herichthys minckleyi*. Ecology 84:1441–1446.

Szedlmayer, S. T., K. W. Able, J. A. Musick, and M. P. Weinstein. 1991. Are scale circuli deposited daily in juvenile weakfish, *Cynoscion regalis*? Environmental Biology of Fishes 31:87–94.

Taylor, E. B., and J. D. McPhail. 2000. Historical contingency and ecological determinism interact to prime speciation in sticklebacks, *Gasterosteus*. Proceedings of the Royal Society B: Biological Sciences 267:2375–2384.

Thibert-Plante, X., and A. P. Hendry. 2009. Five questions on ecological speciation addressed with individual-based simulations. Journal of Evolutionary Biology 22:109–123.

Timelthaler, G. 2010. The crater lake cichlids of Cameroon: visual ecology, opsin molecular evolution and implications for sympatric speciation. Poster presented at Evolution 2010, Society for the Study of Evolution annual conference, Portland, OR, June 25–29.

Trewavas, E., J. Green, and S. A. Corbet. 1972. Ecological studies on crater lakes in West Cameroon: fishes of Barombi Mbo. Journal of Zoology (London) 167:41–95.

Turelli, M. 1988. Phenotypic evolution, constant covariances, and the maintenance of additive variance. Evolution 42:1342–1347.

Turelli, M., N. H. Barton, and J. A. Coyne. 2001. Theory and speciation. Trends in Ecology & Evolution 16:330–343.

Van Doorn, G. S., P. Edelaar, and F. J. Weissing. 2009. On the origin of species by natural and sexual selection. Science 326:1704–1707.

Via, S. 2000. Sympatric speciation in animals: the ugly duckling grows up. Trends in Ecology & Evolution 16:381–390.

———. 2009. Natural selection in action during speciation. Proceedings of the National Academy of Sciences of the USA 106(suppl. 1):9939–9946.

Vonlanthen, P., D. Bittner, A. G. Hudson, K. A. Young, R. Muller, B. Lundsgaard-Hansen, D. Roy, S. Di Piazza, C. R. Largiader, and O. Seehausen. 2012. Eutrophication causes speciation reversal in whitefish adaptive radiations. Nature 482:357–363.

Wilson, D. S., and M. Turelli. 1988. Stable underdominance and the evolutionary invasion of empty niches. American Naturalist 127: 835–850.

Associate Editor: Daniel I. Bolnick
Editor: Mark A. McPeek

Volcanic crater lake Barombi Mbo (*top*), Lake Ejagham (*center*), and one of the six cichlid fishes endemic to Ejagham: *Sarotherodon lamprechti* (*bottom*). Photographs by Christopher Martin.